Optical and Quantum Electronics (2023) 55:1028
https://doi.org/10.1007/s11082-023-05274-x

Optical properties of periodically and aperiodically nanostructured p-n junctions

Z. Taliashvili[1] · E Łusakowska[2] · S. Chusnutdinow[2] · A. Tavkhelidze[3] · L. Jangidze[3] · S. Sikharulidze[1] · Nima E. Gorji[4] · Z. Chubinidze[1] · R. Melkadze[1]

Received: 22 January 2023 / Accepted: 5 August 2023 / Published online: 20 September 2023

Abstract
Recently, semiconductor nanograting layers have been introduced and their optical properties have been studied. Spectroscopic ellipsometry has shown that nanograting significantly modifies the dielectric function of c-Si layers. Photoluminescence spectroscopy reveals the emergence of an emission band with a remarkable peak structure. It has been observed that nanograting also alters the electronic and magnetic properties. In this study, we investigate the quantum efficiency and spectral response of Si p-n junctions fabricated using subwavelength grating layers and aperiodically nanostructured layers. Our findings indicate that the quantum efficiency and spectral response are enhanced in the case of nanograting p-n junctions compared to plain reference junctions. Aperiodically nanostructured junctions exhibit similar results to nanograting junctions. However, aperiodic nanostructuring is a more straightforward fabrication method and, consequently, more appealing for the solar cell industry.

Keywords Nanograting · Quantum efficiency · Spectral response · p-n junction

1 Introduction

The latest advancements in nanotechnology have facilitated the production of submicron periodic nanostructures (Chauvin et al. 2017; Li et al. 2018; Buhl et al. 2021), including 1D and 2D nanogratings. The introduction of such periodic nanostructures has been shown to have a significant impact on the optical properties (Sarnet et al. 2012; Torres et al. 2010; Halbwax et al. 2008; Oh et al. 2012), electronic properties (Vorobyev and Guo 2011; Tavkhelidze et al. 2017, 2021a, b), and other characteristics (Kakulia et al. 2016; Tavkhelidze et al. 2019, 2021a, b) of materials, particularly when the dimensions of the nanogratings (a and w in Fig. 1) are comparable to the wavelength of electrons (de Broglie wavelength). Due to the boundary conditions imposed by the nanograting (NG) on the wave function, certain quantum states (Kakulia et al. 2016) are prohibited, resulting in a reduction in their density of states (DOS).

Extended author information available on the last page of the article

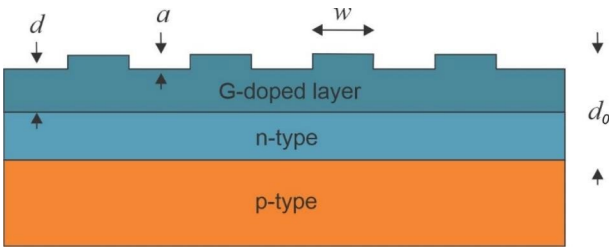

Fig. 1 Nanograting on a substrate surface and the induced layer with reduced DOS.

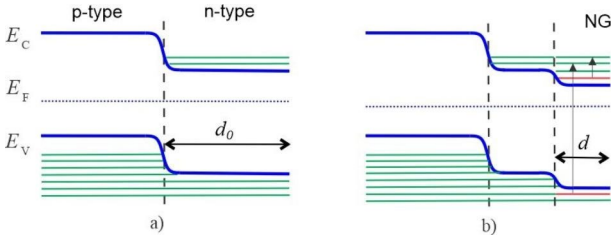

Fig. 2 Schematic energy-band diagrams of an NG layer fabricated on the surface of p-n junction. (a) energy levels of p-n junction; (b). energy levels of p-n junction after nanograting formation. Green lines depict occupied energy levels and red ones are forbidden energy levels. For simplicity, the band gap is scaled down and the energy levels are shown to be equidistant

This phenomenon is commonly known as the geometry-induced quantum effect. In the vicinity of the nanograting (NG) with a layer of thickness d, the density of states (DOS) is reduced (Fig. 1). The boundary conditions imposed by the NG only affect the wave functions of electrons in close proximity to the surface. Conversely, electrons that are further away from the surface experience decoherence. This decoherence arises from the loss of coherence during scattering events, rendering the influence of the grating boundary conditions negligible.

Figure 1 depicts a nanograting (NG) situated on top of an n-type layer (with a thickness of d_0) that forms a p-n junction on the surface of a p-type semiconductor wafer. Figure 2 presents a schematic energy-band diagram of a p-n junction featuring NG patterns. In the immediate vicinity of the NG, certain energy levels within the valence band and conduction band become prohibited. As a result, the excluded electrons tend to occupy only the allowed energy levels shown by green line in Fig. 2.

The higher energy levels at the bottom of the conduction band are occupied by the rejected electrons in the close proximity of the nanograting (NG) layer. This results in an increased concentration of electrons in the conduction band, a phenomenon known as geometry-induced doping or G-doping (Tavkhelidze et al. 2017). In Fig. 2b, it is illustrated that electrons are excluded from both the valence and conduction bands near the NG and are pushed towards the high energy levels in the conduction band. As the Fermi energy increases due to G-doping, it can be considered equivalent to donor doping. G-doping leads to an elevation of the Fermi energy in the vicinity of the nanograting. Importantly, the rejected electrons remain confined to the NG layer. Charge neutrality prohibits the deeper penetration of charges into the substrate, thereby binding the carriers to the characteristic depth d, as depicted in Fig. 2b.

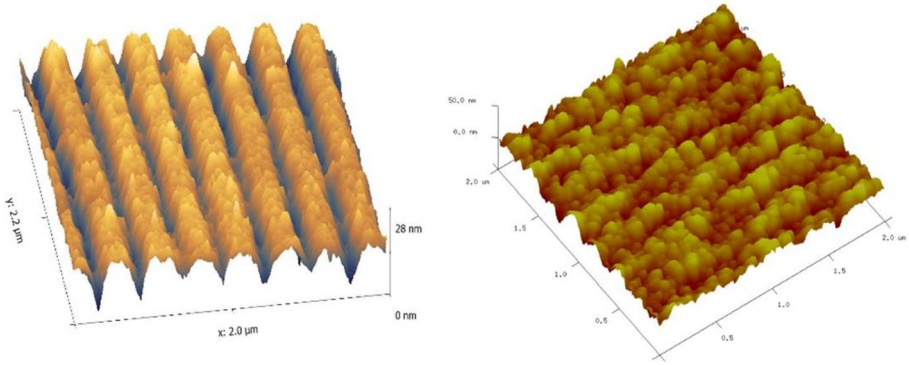

a) b)

Fig. 3 **(a)** AFM scan of nanograting; **(b)** AFM scan of aperiodic structure

Various phenomena associated with geometry-induced quantum effects have been previously documented in different configurations of periodic nanostructures. These effects have been observed in disordered nanostructures generated through wet-etching of p-Si (Luchenko et al. 2016), as well as in nearly periodic nanostructures formed via laser radiation interaction or Laser-Induced Periodic Surface Structures (LIPSS) on surfaces of various semiconductor materials (Mastellone et al. 2022; Edgar et al. 2019; Shuleiko et al. 2021; Nie et al. 2014a, b; Daniel Puerto et al. 2016), metals (Gnilitskyi et al. 2017), indium tin oxide (Ma et al. 2021), and graphene oxide (Mortazavi et al. 2020) layers. Substantial increases in conductivity (n-type conductivity) have been observed in ZnO crystals following the formation of nanoparticles on their surfaces (Nie et al. 2014a, b). Significant alterations in optical properties have been observed in nanograting fused silica materials (Zhou 2016), where spectroscopic ellipsometry measurements have indicated a metallic-type dielectric function (Sarnet et al. 2012; Torres et al. 2010). Strong photoluminescence spectra have been recorded from nanograting surfaces of Si layers (Sarnet et al. 2012; Halbwax et al. 2008). It is noteworthy that the photoluminescence phenomenon is observed in indirect band gap materials such as Si. In our measurements on nanograting (NG) samples, we have observed additional periodic peaks in the photoluminescence spectrum, and the positions of these peaks align with the predictions of the geometry-induced doping (G-doping) theory.

In this study, we present the fabrication of c-Si p-n junction samples incorporating subwavelength gratings and aperiodic nanostructuring, and investigate their optical characteristics, including quantum efficiency and spectral response.

2 Sample preparation and characterization

For sample preparation, p-type silicon<100>substrates with resistivity ranging from 1 to 10 Ω·cm were utilized. The standard technology for p-n junction formation was employed. Phosphorus donor atoms were diffused into the top layer at a temperature of 1050 °C for a duration of 5–7 min, resulting in a diffusion depth of 200-250 nm. The obtained large-area

p-n junctions served as the basis for the fabrication of nanograting and aperiodically nanostructured samples. These p-n junctions also served as reference plain samples.

To create the nanograting patterns on the surface of silicon substrates, laser interference lithography and subsequent reactive ion etching were employed, resulting in nanogratings with a depth of 20–30 nm and a period of 300 nm (Tavkhelidze et al. 2017). A nanograting area of 3 mm x 3 mm was fabricated in the center of a 10 mm x 10 mm chip.

To prepare the samples for interference lithography, the following steps were undertaken:

The substrates were treated in a solution of H2SO4 + H2O2 + H2O (1:1:3) for 5–10 min. They were then cleaned in deionized water for 10 min and dehydrated using a centrifuge. The substrates were passivated in HF + H2O (1:20) and rinsed in deionized water for 10 min. Dehydration was performed again using a centrifuge and a hotplate at 180 °C for 20 min. A negative photoresist (ma-N 2401) was applied at a speed of 4000–4200 rpm for 30 s, resulting in a resist thickness of 70-90 nm. Finally, the resist was dried at 90–115 °C for 10 min.

For laser interference lithography, a Blue-Violet (375 nm) semiconductor laser DL375-010-SO with a coherence length of over 20 m was used as the light source (Tavkhelidze et al. 2017; Shimizu 2021; Reif et al. 2006). The interference fringe width ranged from 140 to 1000 nm. The resist was exposed for 10–25 s and then developed in an alkaline solution (AZ-400 K + H2O, 1:3) for 20–35 s.

Reactive ion etching (RIE) was conducted using a homemade setup within a vacuum chamber, along with DC magnetrons. CF4 gas was used at a pressure of P = 6-7 × 10-2 Pa, voltage V = 3.8–4.2 kV, and current I = 200 mA. The etching time varied from 6 to 20 min, depending on the desired etching depth. A negative photoresist layer was employed during interference lithography to ensure uniform etching of the entire chip's surface, including the reference plain area, as done in previous works (Tavkhelidze et al. 2021a, b). This step was taken to eliminate the influence of reactive ion etching through comparison with the reference area. To control the nanograting depth, an on-chip step structure was utilized and measured using a profilometer. The surface roughness after etching did not exceed RMS = 1 nm.

For the creation of aperiodic nanostructures, the MacEtch technology, specifically the Ag nanoparticle-based technology (Ag-MacEtch) (Hee et al. 2014; Nichkalo et al. 2017), was employed. An adhesive solution consisting of AgNO3 + HF with Ag nanoparticles of 100-150 nm diameter was prepared. The backside-protected Si substrate was immersed in the adhesive solution at room temperature for 10–20 s. Subsequently, following a standard cleaning procedure, the wafer with the large-area p-n junction was immersed in an HF + H2O2 solution for Si etching. The etching rate was 1.1 nm/second. Finally, Ag nanoparticles in an HNO3 solution were used.

Surface morphology was examined using an AFM (Atomic Force Microscopy) Bruker Dimension Icon, while the quantum efficiency and spectral response were measured using the solar cell parameter control system Rera Solutions SpeQuest.

In Fig. 3(a), a typical AFM scan of the nanograting is presented. The shape of the grating cross-section was observed to be slightly disproportional and occasionally sinusoidal, consistent with our previous studies (Torres et al. 2010; Tavkhelidze et al. 2017, 2019), which is characteristic of laser interference lithography. Based on the AFM image, the depth of the nanograting ranged from 20 to 30 nm, and the lateral period was 2w = 300 nm. As a reference, we also prepared a continuous, un-patterned (plain) Si layer on the same substrate, which underwent the same reactive ion etching process to eliminate any influence from RIE.

Figure 3(b) displays a typical AFM scan of an aperiodic nanostructure. The depth of the structure varies between 20 and 30 nm, and its morphology appears quite irregular.

3 Results and discussion

The responsivity spectra (SR) and quantum efficiency (QE) of the p-n Si junction with nanograting and aperiodic nanostructures in the n-type layer of the p-n junction were measured at room temperature and are presented in Figs. 4 and 5, respectively. The depth of the structures varies across the measured area and has an average value of 20 nm for both the nanograting and aperiodic structures. The diodes were illuminated through the top layer of the n-type Si.

The devices exhibit photosensitivity in the visible spectral region, covering wavelengths from approximately 350 nm up to 1100 nm. From the presented figures, it is evident that the signal intensity strongly depends on the surface texture. The devices with the textured surface show higher photovoltaic signal intensity throughout the wavelength range. This leads to an increase in SR and QE, as indicated by the green curves in Figs. 4 and 5.

For both the nanograting and aperiodic structures, the increase in QE is estimated to be around 25% compared to reference structures without a textured surface (plain p-n junction). It is worth noting that no surface grinding or any extra partner materials (as anti-reflection layer) were utilized in these measurements.

In both cases of nanograting and aperiodic nanostructures, the maximum increase in QE and SR occurs within the wavelength range of 600 to 900 nm. This effect is distinct from the photoluminescence observed in quantum dots and other nanostructures with sizes on the order of a few nanometers. For instance, silicon quantum dots exhibit photoluminescence despite the material's indirect band gap (Lu et al. 2017).

To ensure that the observed increase in QE and SR is not influenced by photoluminescence or other factors, we conducted reactive ion etching on both the plain reference samples and the nanograting samples. This ensures the presence of defects introduced by the reactive ion etching process in the reference samples as well. The observed photoluminescence in G-doped layers may contribute to the increase in QE and SR.

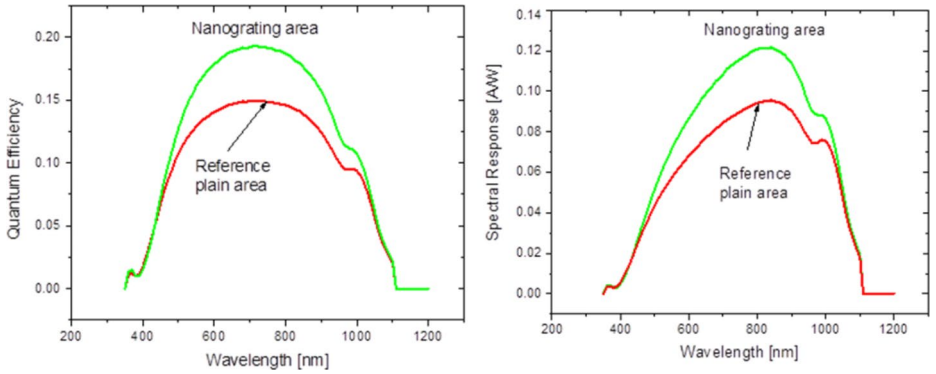

Fig. 4 QE and SR of nanograting sample. Green curves correspond to nanograting area. Red curves correspond to adjacent plain (reference) area

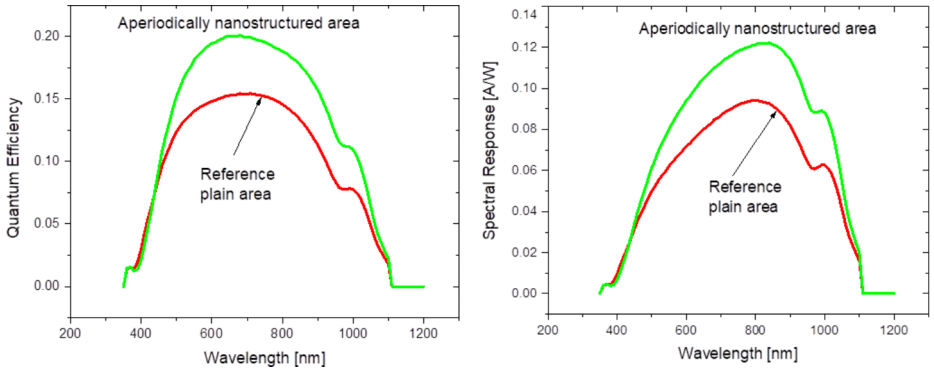

Fig. 5 QE and SR of aperiodically structured sample. Green curves correspond to aperiodic nanostructure area. Red curves correspond to adjacent plain (reference) area

There is a slight difference in the spectra of the nanograting and aperiodic nanostructures. The maxima of QE in the aperiodic structure exhibit a minor blue shift (Fig. 5), which can be attributed to electromagnetic wave scattering.

The significant increase (25%) in QE and SR can be attributed to the changes in the optical properties of the Si material, specifically the reduction of DOS (density of states). This reduction in DOS affects the interband density of states and subsequently alters the optical properties of the material. This observation aligns with our previous findings of substantial changes in the dielectric function (Sarnet et al. 2012) and the emergence of a new and intense photoluminescence band (Halbwax et al. 2008) in nanostructured Si.

Moving forward, our plan is to fabricate prototypes of solar cells utilizing nanostructured junctions and investigate their efficiency as a function of nanostructuring. This research aims to further explore the potential benefits of incorporating nanostructures in solar cell designs and evaluate their impact on overall solar cell performance.

4 Conclusions

On Si substrates, large area p-n junctions were fabricated. The n-type top layer was nanostructured using subwavelength nanograting and aperiodic structures. Quantum efficiency and spectral response were studied. The results revealed that the nanograting device exhibited a significant increase of up to 25% in both quantum efficiency and spectral response compared to the reference plain device. This improvement can be attributed to geometry-induced quantum effects, which alter the dielectric function of Si and induce strong photoluminescence in the indirect band gap material. Interestingly, the aperiodically nanostructured junction showed similar results to the nanograting device. However, aperiodic nanostructuring offers the advantage of being easier to fabricate, making it more attractive for the solar cell industry. In the next phase, prototypes of solar cells based on nanostructured junctions will be fabricated, and their efficiency dependence on nanostructuring will be thoroughly investigated in future studies.

Acknowledgements Authors thank G. Skhiladze, A. Bibilashvili, N. Kitoshvili, M. Mebonia for discussions and support.

Author contributions Z. T.: methodology, experimental research; E. L. : optical measurements; S. C. : optical measurements, A.T.: concept, manuscript writing,; L. J. : technology, chemistry; S. S.: technology; N. G. : manuscript review; Z. C. : experimental setup; R. M. measurements

Funding Research was partly funded by Shota Rustaveli National Science Foundation (SRNSF) and Georgia National Innovation Ecosystem, grant number CARYS-19-218.
Open Access funding provided by the IReL Consortium

Data Availability No dataset was used in this manuscript. Any data or materials can be provided by personal contact to corresponding author.

Declarations

Competing interests Authors declare NO conflict of interests in financial or personal nature.

Ethical approval Not applicable.

References

Buhl, J., Yoo, D., Köpke, M., Gerken, M.: Two-Dimensional Nanograting fabrication by Multistep Nanoimprint Lithography and Ion Beam Etching. Nanomanufacturing. **1**, 39–48 (2021). https://doi.org/10.3390/nanomanufacturing1010004

Chauvin, A., Stephant, N., Du, K., Ding, J., Wathuthanthri, I., Choi, C.-H., Tessier, P.-Y., Mel, E.,, A.-A.: Large-scale fabrication of porous gold nanowires via laser interference lithography and dealloying of gold–silver Nano-Alloys. Micromachines. **8**, 168 (2017). https://doi.org/10.3390/mi8060168

Daniel Puerto, M., Garcia-Lechuga, J., Hernandez-Rueda, A., Garcia-Leis: Santiago Sanchez-Cortes, Javier Solis and Jan Siegel, Femtosecond laser-controlled self-assembly of amorphous-crystalline nanogratings in silicon. Nanotechnology. **27**, 265602 (2016)

Edgar, G.-F., Álvaro Rodríguez-Rodríguez, Mari-Cruz García-Gutiérrez, Nogales, A., Ezquerra, T.A.: Esther Rebollar, Functional nanostructured surfaces induced by laser on fullerene thin films, Applied Surface Science, Volume 476, Pages 668–675, (2019). https://doi.org/10.1016/j.apsusc.2019.01.141

Gnilitskyi, I., Derrien, T.J.Y., Levy, Y., et al.: High-speed manufacturing of highly regular femtosecond laser-induced periodic surface structures: Physical origin of regularity. Sci. Rep. **7**, 8485 (2017). https://doi.org/10.1038/s41598-017-08788-z

Halbwax, M., Sarnet, T., Delaporte, P., Sentis, M., Etienne, H., Torregrosa, F., Vervisch, V., Perichaud, I., Martinuzzi, S.: Micro and nano-structuration of silicon by femtosecond laser: Application to silicon photovoltaic cells fabrication. Thin Solid Films. **516**, 6791–6795 (2008)

Hee, H., Zhipeng, H., Woo, L.: Metal-assisted chemical etching of silicon and nanotechnology applications. Nano Today. **9**, 3, 271–304 (2014)

Kakulia, D., Tavkhelidze, A., Gogoberidze, V., Mebonia, M.: Density of quantum states in quasi-1D layers. Phys. E. **78**, 49 (2016). https://doi.org/10.1016/j.physe.2015.11.033

Li, H., Wang, X., Zhu, X., Duan, X., Pan, A.: Composition modulation in one-dimensional and two-dimensional chalcogenide semiconductor nanostructures. Chem. Soc. Rev. **47**, 7504 (2018)

Lu, S., Wu, B., Sun, Y., Cheng, Y., Liao, F., Shao, M.: Photoluminescence of pure silicon quantum dots embedded in an amorphous silica wire array. J. Mater. Chem. C. **5**, 6713–6717 (2017)

Luchenko, A.I., Melnichenko, N., Svezhentsova, K.V.: Local Electronic Properties of the Surface of the Nanostructured Silicon Layers. In Proceedings of the 2016 IEEE 36th International Conference on Electronics and Nanotechnology (ELNANO), Kyiv, Ukraine, 19–21 April ; p. 43. (2016)
Ma, H., Zhao, Y., Shao, Y., Lin, X., Li, D., Cao, Z., Leng, Y., Shao, J.: Determining femtosecond laser fluence for surface engineering of transparent conductive thin films by single shot irradiation. Opt. Express. **29**(23), 38591–38605 (2021). https://doi.org/10.1364/OE.442882 PMID: 34808909
Mastellone, M., Pace, M.L., Curcio, M., Caggiano, N., De Bonis, A., Teghil, R., Dolce, P., Mollica, D., Orlando, S., Santagata, A., Serpente, V., Bellucci, A., Girolami, M., Polini, R., Trucchi, D.M.: LIPSS Applied to Wide Bandgap Semiconductors and Dielectrics: Assessment and Future Perspectives, Materials 15, 1378. (2022). https://doi.org/10.3390/ma15041378
Mortazavi, S., Mollabashi, M., Barri, R., Gundlach, L., Jones, K., Xiao, J.Q., Oplia, R.L., Shah, S.I., Ti: Sapphire laser irradiation of graphene oxide film in order to tune its structural, chemical and electrical properties: Patterning and characterizations. Appl. Surf. Sci. **500**, 144053 (2020)
Nichkalo, S., Druzhinin, A., Evtukh, A., Bratus', O., Steblova, O.: Silicon Nanostructures produced by modified MacEtch Method for Antireflective Si Surface. Nanoscale Res. Letters. **12**, 106 (2017). https://doi.org/10.1186/s11671-017-1886-2
Nie, M., Zhao, Y., Zeng, Y.: Effects of annealing and laser irradiation on optical and electrical properties of ZnO thin films. J. LASER Appl. VOLUME. **26**, 022005–022001 (2014a)
Nie, M., Zhao, Y., Zeng, Y.: Effects of annealing and laser irradiation on optical and electrical properties of ZnO thin films. J. Laser Appl. **26**, 022005 (2014b)
Oh, J., Yuan, H.-C., Branz, H.M.: An 18.2% efficient black-silicon solar cell achieved through control of carrier recombination in nanostructures. Nat. Nanotechnol. **7**, 743–748 (2012)
Reif, J., Ratzke, M., Varlamova, O., Costache, F.: Electrical properties of laser-ablation-initiated self-organized nanostructures on silicon surface. Mater. Sci. Eng., B. **134**, 114–117 (2006)
Sarnet, T., Carey, J.E., Mazur, E.: From black silicon to photovoltaic cells, using short pulse lasers, AIP Conference Proceedings, 1464, 219. (2012)
Shimizu, Y.: Laser interference lithography for fabrication of Planar Scale Gratings for Optical Metrology. Nanomanuf. Metrol. **4**, 3–27 (2021)
Shuleiko, D., Martyshov, M., Amasev, D., Presnov, D., Zabotnov, S., Golovan, L., Kazanskii, A., Kashkarov, P.: Fabricating Femtosecond Laser-Induced Periodic Surface Structures with Electrophysical Anisotropy on Amorphous Silicon. Nanomaterials. **11**, 42 (2021)
Tavkhelidze, A., Jangidze, L., Mebonia, M., Piotrowski, K., Więckowski, J., Taliashvili, Z., Skhiladze, G., Nadaraia, L.: Geometry induced quantum effects in periodic nanostructures. Phys. Staus Solidi A. **214**, 1700334 (2017). https://doi.org/10.1002/pssa.201700334
Tavkhelidze, A., Grabecki, G., Jangidze, L., Yahniuk, I., Taliashvili, Z., Taliashvili, B.: Negative Magnetoresistance in Si Nanograting Layers. Phys. Status Solidi A. **216**, 1800693 (2019). https://doi.org/10.1002/pssa.201800693
Tavkhelidze, A., Bibilashvili, A., Jangidze, L., Gorji, N.E.: FermI–level tuning of G-doped layers. Nanomaterials. **11**, 505 (2021a). https://doi.org/10.3390/nano11020505
Tavkhelidze, A., Jangidze, L., Taliashvili, Z., Gorji, N.E.: Metal-Semiconductor Junction Coatings. **11**, 945 (2021b). https://doi.org/10.3390/coatings11080945 G-Doping-Based
Torres, R., Vervisch, V., Halbwax, M., Sarnet, T., Delaporte, P., Sentis, M., Ferreira, J., Barakel, D., Bastide, S., Torregrosa, F., Etienne, H., Roux, L.: Femtosecond laser texturization for improvement of photovoltaic cells: Black Silicon. J. Optoelectron. Adv. Mater. **12**, 3 (2010)
Vorobyev, A., Guo, C.: Antireflection effect of femtosecond laser-induced periodic surface structures on silicon. Opt. Express. **19**, A1031–A1036 (2011)
Zhou, F.: Yuan'an Zhao, Jianda Shao, Femtosecond laser-induced periodic surface structure on fused silica surface. Optik. **127**, 1171–1175 (2016)

Authors and Affiliations

Z. Taliashvili[1] · E Łusakowska[2] · S. Chusnutdinow[2] · A. Tavkhelidze[3] · L. Jangidze[3] · S. Sikharulidze[1] · Nima E. Gorji[4] · Z. Chubinidze[1] · R. Melkadze[1]

✉ Nima E. Gorji

nima.gorji@tudublin.ie

Z. Taliashvili
ztaliashvili@gmail.com

E Łusakowska
lusake@ifpan.edu.pl

S. Chusnutdinow
chusnut@ifpan.edu.pl

A. Tavkhelidze
avtandil.tavkhelidze@iliauni.edu.ge

L. Jangidze
larisajangidze@gmail.com

S. Sikharulidze
sixarulidze1944@gmail.com

[1] Institute of micro and nano electronics, Chavchavadze Ave, Tbilisi, Georgia

[2] Institute of Physics, Polish Academy of Sciences, Al. Lotników, Warsaw, Poland

[3] Center of Nanotechnology for Renewable Energy, Ilia State University, Tbilisi, Georgia

[4] School of Mechanical Engineering, Technological University Dublin, Dublin, Ireland